Available online at www.sciencedirect.com

ScienceDirect

Physics Procedia 67 (2015) 840 – 846

Physics Procedia

25th International Cryogenic Engineering Conference and the International Cryogenic Materials Conference in 2014, ICEC 25–ICMC 2014

Quench modeling in high-field Nb_3Sn accelerator magnets

S. Izquierdo Bermudez*, H. Bajas, L. Bottura

CERN, CH-1211 Geneva 23, Switzerland

Abstract

The development of high-field magnets is on-going in the framework of the LHC luminosity upgrade. The resulting peak field, in the range of 12 T to 13 T, requires the use Nb_3Sn as superconductor. Due to the high stored energy density (compact winding for cost reduction) and the low stabilizer fraction (to achieve the desired margins), quench protection becomes a challenging problem. Accurate simulation of quench transients in these magnets is hence crucial to the design choices, the definition of priority R&D and to prove that the magnets are fit for operation. In this paper we focus on the modelling of quench initiation and propagation, we describe approaches that are suitable for magnet simulation, and we compare numerical results with available experimental data.

Peer-review under responsibility of the organizing committee of ICEC 25-ICMC 2014

Keywords: Quench simulation; Superconducting magnets; Nb_3Sn superconductor; accelerator magnets

1. Introduction

Quench protection of high-field Nb_3Sn accelerator magnets for the LHC luminosity upgrade, and specifically the 11 T dipole for the LHC Dispersion Suppressor [1], and the Interaction Region quadrupoles QXF [2], is a critical aspect. The peak field required by design, ranging around 12 T to 13 T in both 11 T and QXF, and the large magnet aperture, e.g. 150 mm diameter for the QXF, result in a stored energy density well in excess of 150 MJ/m^3, i.e. nearly a factor three with respect to the present LHC dipoles run at nominal field, at approximately 60 MJ/m^3. It is

* Corresponding author. Tel.: +41-22-767-6222; fax: +41-22-767-6300.
E-mail address: susana.izquierdo.bermudez@cern.ch

Peer-review under responsibility of the organizing committee of ICEC 25-ICMC 2014
doi:10.1016/j.phpro.2015.06.141

clear that in this regime it is of paramount important to detect rapidly the quench, and the magnet needs to be actively and reliably protected by heaters. Given the little margin, the detailed understanding of the thermodynamic processes during a quench is hence crucial for the design of the essential protective elements. The main concerns are the detection of the quench once the initial normal zone propagates along the conductor, the delay to induce a distributed quench using quench heaters or comparable mechanism and the time need for the quench to propagate throughout the whole magnet cross section.

Accurate quench modeling is a challenging problem mainly due to the large disparity of time scales and length scales and the highly non-linear nature of the quench process, meaning that slightest numerical errors can rapidly grow to unacceptable limits [3,4]. The details of simulation of quench propagation along a conductor are generally mastered [5,6]. For this reason we focus here on the thermal coupling between parallel conductors. In principle, for an adiabatic winding, the process is described in detail by the transient, non-linear 3-D heat balance equation. Our aim is to develop a fast algorithm to apply the code for quench simulations in large magnet systems simplifying the 3D problem by a set of 1D longitudinal continuum models for the conductor and a 2-D heat conduction model for the insulation.

2. Description of the model

As anticipated, the basic model of heat transfer within the coil is based on the 1D solution for quench initiation and propagation along the conductor (the winding direction), thermally coupled across the winding in different manners, as discussed below. This approach was adopted for solenoids [7-10] and fusion magnets [11-12]. A conductor is assumed to be made of components (e.g. the cable, the insulation), the *i*-th component having a temperature T_i. We write the 1D heat transport equation along the winding direction for each of the components, in the hypothesis of an adiabatic winding (i.e. no heat transfer to the helium bath during the time scale of interest for a magnet quench), as follows:

$$\sum_k A_k \rho_k C_k \frac{\partial T_i}{\partial t} - \frac{\partial}{\partial x}\left(\sum_k A_k k_k \frac{\partial T_i}{\partial x} \right) = \sum_j H_{ij}\left(T_j - T_i\right) + \dot{q}_i + \dot{q}_{Joule,i} + \dot{q}_{adj,i}\,, \tag{1}$$

where A_k, ρ_k, C_k and k_k are, respectively, the cross section, density, specific heat and conductivity of the *k*-th constituent of the component itself (e.g. Nb_3Sn, Copper, and barriers in the strands of the cable). $\dot{q}_i$ is the external heat perturbation power per unit length, $\dot{q}_{Joule,i}$ is the Joule heat power per unit length, $\dot{q}_{adj,i}$ is the power exchange between adjacent conductors, and $H_{ij}(T_i-T_j)$ is the power exchanged between components *i* and *j* in the conductor across the thermal conductance H_{ij}. Note that some of these terms can be nil for a component, but the equation is retained in full form for generality.

In Eq. (1), the 3D part of the problem, the transverse heat exchange, is concentrated in the adjacent heat exchange among conductors $\dot{q}_{adj,i}$. Two approaches are investigated for the transverse power exchange. The first approach is based on a simplified 2D network model. This approximation is good for situations when the temperature gradient across the insulation is in steady state. In the second approach, the heat conduction in the insulation is solved using a finite element mesh and is thermally coupled to the conductor in a number of selected “cuts”. This approach allows for more freedom in the description of temperature gradients in all winding directions.

2.1. 1D longitudinal model

To solve the general 1D heat transport equation we use the multi-physics model THEA (Thermal, Hydraulic and Electric Analysis of Superconducting Cables [13]). For simplicity, in this study the hydraulic and electric part of the model has been dropped, focusing on the thermal phenomena. Details are described in [6]. The conductor is modeled separating the cable and its insulation in two thermal components at different temperature. Each component, in turn, can have an internal composite material structure. For instance, the cable itself is composed of the superconductor and the copper stabilizing matrix. The state of the materials in each component (e.g. temperature, field, strain) is uniform, the material properties are homogenized based on area or density averages, as appropriate,

and the current is distributed in accordance to the resistivity of each material. The degree of thermal separation among components depends on the thermal conductance H_{ij} among them. As discussed later, this thermal contact is not well known, and we will consider values ranging from one extreme of complete insulation (i.e. cable only) to the opposite extreme of perfect thermal contact (i.e. cable and insulation at identical temperature).

The model available in THEA solves implicitly in space (finite elements) and time (multi-step finite differences) a set of equations of the prototype Eq. (1), resulting in linear unconditional stability. The advantage of this 1D model is the possibility of using an adaptive mesh algorithm [5] that allows a mesh size in the range of 0.1mm to 1mm at the propagation front, while a coarse mesh can be used in the rest of the magnet, enabling the simulation of a full magnet with acceptable requirements from the point of view of memory and CPU time.

2.2. First approach: 2D transverse thermal network

To a first approximation, the transverse heat flux in the composite formed by a cable and its insulation can be described using a thermal resistance analogy. This is illustrated in Fig. 1, schematically showing the analogy of conductors in thermal contact in the cross section of a typical accelerator magnet, and a thermal network between the conductors. Note that each conductor has been separated into cable and insulation, as discussed above.

Three types of thermal contacts can be identified: adjacent conductors n and m in the same layer (thermal conductance H_{nm}), adjacent conductors n and l in different layers (thermal conductance H_{nl}), and a thermal contact to the helium bath (thermal conductance H_{bath}). The heat flux between adjacent conductors n and m is given by:

$$\dot{q}_{adj,i} = H_{nm}(T_{i,m} - T_{i,n}), \tag{2}$$

and the other heat flux types follow by analogy. Several levels of approximation are possible in the thermal network. The one shown above already contains two temperature gradients (within the conductor and across the insulation). It can be further simplified if the internal thermal conductance in the conductor (H_{ij}) is large, resulting in a single thermal resistance, between adjacent conductors, which is lumping the effect of the whole insulation thickness. Increasing resolution, and complexity, could be achieved by increasing the subdivision of the insulation. We discuss the level of approximation later.

In this work, the coupling between the 1D conductor and insulation model and the transverse thermal network is done using an explicit formulation, i.e. the heat flux at time step t is computed based on values of temperature at time step t-1:

$$\dot{q}^{t}_{adj,i} = H^{t-1}_{nm}(T_{i,m}{}^{t-1} - T_{i,n}{}^{t-1}). \tag{3}$$

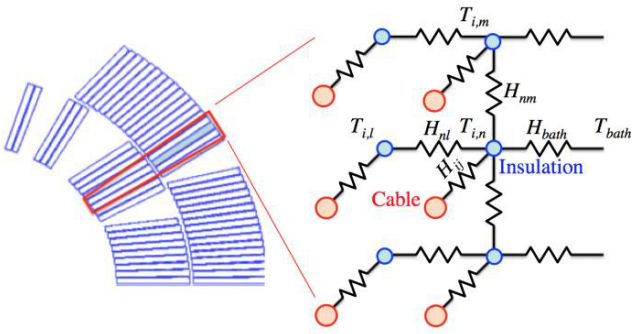

Fig. 1. Analogy of conductors in thermal contact in the cross section and a thermal network between the conductors.

This heat source is then added to the 1D heat equation of the insulation with no iteration or correction of the temperature variation. This is the simplest way to introduce heat fluxes but it is conditionally stable, so the time step should be sufficiently small to converge [4]. Note, finally, that the calculation of the transverse heat transfer must deal with the fact that the model of a developed conductor does not have matching nodes in the 1D mesh locations where conductors are adjacent across the coil winding. This is resolved by an interpolation of the temperatures using the linear finite element shape functions at the location of the coupling.

2.3. Second approach: 2D transverse finite element mesh

In the second approach, the 3D problem of heat conduction in the insulation is modeled by approximating it with a series of 2D problems to be solved on a number of "cuts" at selected locations along the winding. On each selected cut, a finite element mesh is generated, giving us the maximum flexibility in describing the details of the system (e.g., insulation layers, quench heaters, etc.). We use 2D quadrilateral elements with four nodes and first order shape function. A sufficient mesh density in the 2D plane is an important parameter required to achieve physical solutions.

Similarly to above, the temperature in the cable is computed by THEA. In this case the insulation is not considered. The temperature of the cable is set as boundary condition in the 2D mesh, at a given "cut". The temperature in the 2D mesh is solved by the finite element code HEATER (Heat conduction [14]) that solves the parabolic heat conduction equation in the insulation. The heat power exchanged across the insulation is then used to compute the $\dot{q}_{adj,i}$ term that enters the 1D heat transfer equation in the conductor. An advantage of this domain decomposition is that each process can advance the time integration based on its own time step. The solution is separately advanced in time over each partition. In this work, the coupling between THEA and HEATER is synchronized by SUPERMAGNET (Multitask Code Manager [15]) interpolating linearly the data made available by each process.

THEA and HEATER use numerical semi-implicit algorithms. This guarantees that the numerical solution of each of the two physical domains, considered separately, is linearly stable [16]. As for the thermal network, this is not the case for the coupling across the two codes, which is fully explicit.

The space convergence of the coupling THEA/HEATER has been investigated by running it with different distances between 2D cuts in the range 10 mm – 200 mm. For distances between cuts longer than $\Delta z = 40$ mm numerical diffusion start to appear. Time integration using Galerkin first order method with adaptive time stepping showed better convergence behavior than other higher order methods. Relative errors at each time step during the time integration process should be lower than $5 \cdot 10^{-4}$ to achieve a numerically stable solution. Improved methods for the convergence of the coupling across the codes could allow the use of longer elements (Δz in the order of hundreds of mm) enabling the simulation of a full magnet with reasonable computing resources.

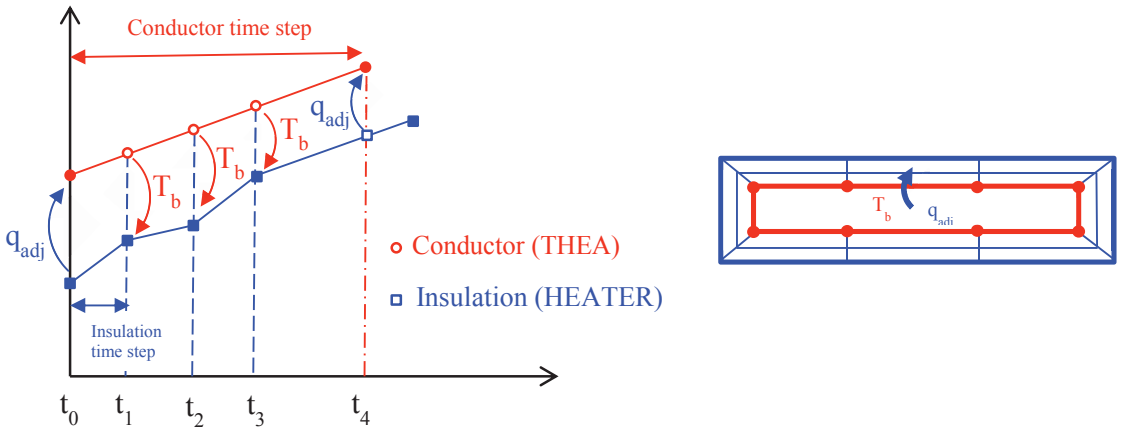

Fig. 2. Schematic representation of the coupling between the conductor (1D longitudinal model) and insulation (2D finite element model).

3. Results and discussion

The model is compared with the experimental data produced in a Short Model Racetrack Coil (SMC) built and tested at CERN [17]. The conductor is made out of 40 strands 0.7 mm diameter. Insulation thickness is 0.15 mm, copper to non-copper ratio 1.25 and the copper residual resistivity ratio is RRR=100. We use the parameterization of critical current proposed in [17] and the magnetic field is computed using the software ROXIE [18].

3.1. Hot-spot temperature

A conservative estimate of the hot spot can be obtained by using the heat balance equation assuming adiabatic conditions and constant magnetic field equal to the peak field in the conductor:

$$\int_0^{\infty} [I(t)]^2 \, dt = A_{total} A_{Cu} \int_{T_0}^{T_e} \frac{C_p^{ave}(T)}{\rho_{Cu}(T)} dT \,, \tag{4}$$

where I is the current in the magnet, A_{total} the cross sectional surface of the cable (including insulation), A_{Cu} is the copper surface, C_p^{ave} the average volumetric specific heat and ρ_{Cu} the copper resistivity. The left-hand side depends only on the response of the circuit and the right-hand side (what we call QI) is a property of the materials in the cable, where one can consider only the conductor or the conductor and the insulation. We study here a specific case for a natural quench starting in the high field region at 13.2 kA. Experimental data defines the temperature in the conductor based on the copper resistivity measurements. Fig. 3 on the right shows that the model predicts a hot spot temperature about 30 K lower than the measured value. The measured temperature is closer to the adiabatic temperature considering only the heat capacity of the conductor. Uncertainties in the initial development of the quench introduce small errors (both in the model and in the experimental data) that can explain the difference observed at the beginning of the quench. The model has been used to explore how the hot spot temperature can vary for the same integral of the square of the current decay depending on the dynamics of the quench. In all the cases, the quench starts in the high field region and the total integral for the square of the current is 13 MA^2s. Differences up to 40 K in the hot spot are observed.

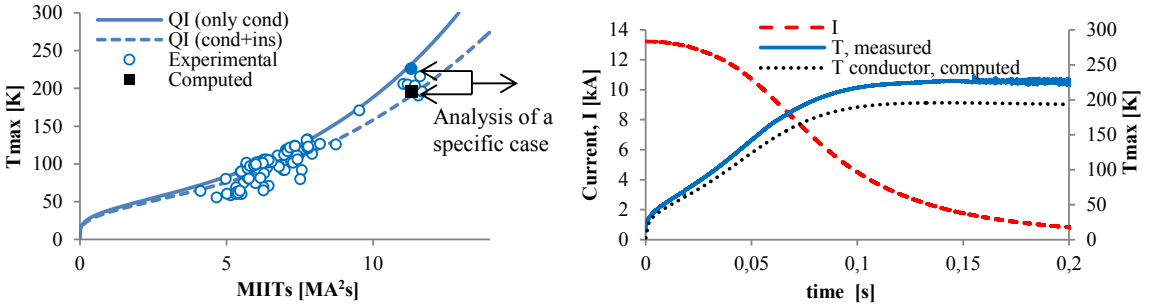

Fig. 3. Left: Measured hot spot temperature at different current levels compared with the adiabatic hot spot. Right: Analysis of a specific case.

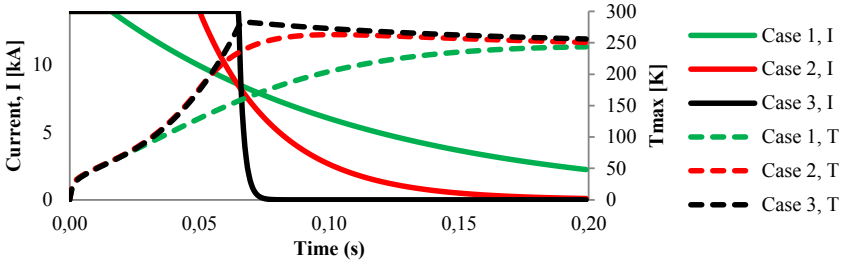

Fig. 4. Current decay and temperature rise in the conductor for three different cases with the same total integral of the square of the current.

3.2. Longitudinal quench propagation

Longitudinal propagation velocity strongly depends on the current density on the copper (Joule heating) and the Current Sharing Temperature (T_{cs}). The field dependence of the material properties is less important, being T_{cs} the dominating factor affected by the field (see Fig. 5). Considering or not the heat capacity of the insulation also has an important impact on the longitudinal quench propagation. Fig. 6 compares the measured propagation velocity with the computed value at different current levels for quenches occurring on the high field region of the magnet. The data becomes more spread at higher currents where the temperature margin is lower and small variations on the current sharing temperature can lead to large changes on the propagation velocity.

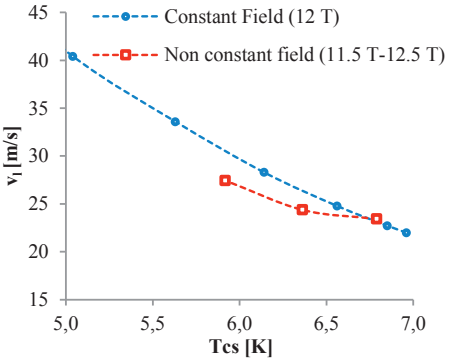

Fig. 5. Impact of the current sharing temperature on the longitudinal quench propagation velocity.

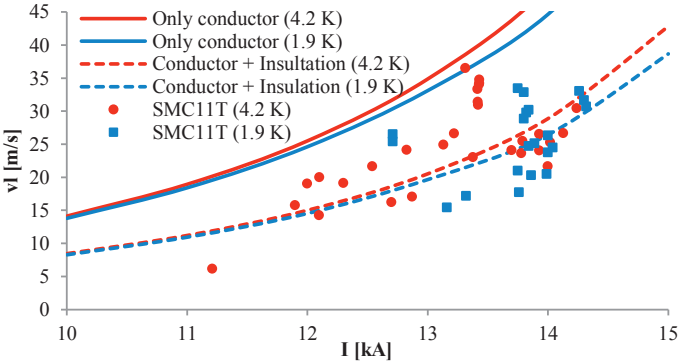

Fig. 6. Computed longitudinal propagation velocity compared to experimental data measured on SMC.

3.3. Transverse quench propagation

The 2D transverse model is the key factor affecting the propagation of the normal zone in the transverse direction. A good discretization of the insulation is particularly important at the beginning of the quench, when the thermal diffusivity is changing very rapidly. Fig. 7 shows that the temperature in the conductor where the quench starts is very close when the transversal heat exchange is modelled using a using a second order thermal network and a finite element mesh. It is not the case for the turn to turn propagation. Fig. 8 shows the temperature distribution in the insulation between adjacent conductors at different times using the two methods for the modelling of the transverse heat transfer. z=0.2 mm represents the location of the turn that is quenching and z=0 mm the adjacent conductor.

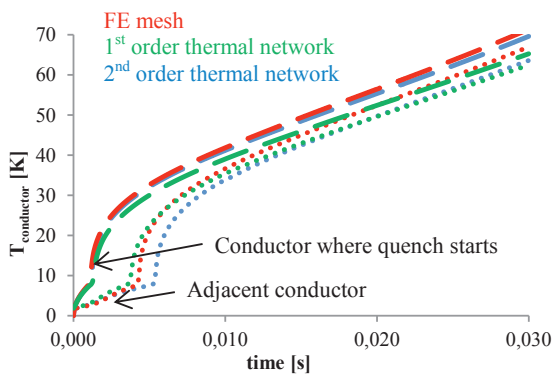

Fig. 5. Temperature in the conductor for a quench at 11.85 kA and 11.3 T field.

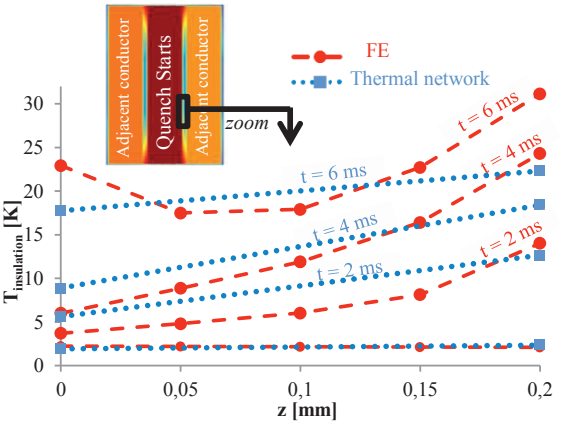

Fig. 6. Temperature profile in the insulation between two adjacent conductors at different times.

4. Conclusion

New accelerator magnets based on Nb_3Sn are pushing the boundary of protection and it is essential to establish a good understanding of the dominating physics. The large disparity of lengths and time scales requires an appropriate subdivision in order to model full magnet systems with reasonable computing resources. A refined 2D transverse model is important to resolve the temperature gradients in the insulation. It has a direct impact on the turn to turn propagation. Hot spot temperature and longitudinal propagation are not significantly affected by the transverse model.

References

1. Karppinen M., *et al.*, Design of 11 T Twin-Aperture Dipole Demonstrator Magnet for LHC Upgrades. IEEE Transaction on Applied Superconductivity, vol. 22, no. 3, June 2013.
2. Ferracin P.**,** *et al*., Magnet Design of the 150 mm Aperture Low-β Quadrupoles for the High Luminosity LHC. IEEE Transaction on Applied Superconductivity, vol. 24, no. 3, June 2014.
3. Bottura L., Shajii A., Numerical quench back in thermo-fluid simulations of superconducting magnets. International Journal for Numerical Methods in Engineering, 43, 1275-1293 (1998)
4. Bottura L., Heller R., Criteria for the numerical convergence of quench simulations in CICCS'S. Cryogenics 46 (2006) 556-562
5. Bottura L. A Numerical Model for the Simulation of Quench in the ITER Magnets. J Comput. Phys. 1996;125:26-41
6. Bottura L, Rosso C, Vreschi M. A general model for thermal, hydraulic and electric analysis of superconducting cables. Cryogenics 2000; 40:617
7. Gavrilin AV. Computer simulation of thermal process during quench in superconducting winding of solenoid. IEEE Trans Appl Supercond 1993;3(1):293–6.
8. Gavrilin AV, Konyukhov AA, Malginov VA. Computer simulation and experimental study of quench in superconducting epoxy-impregnated multilayer coil. IEEE Trans Mag 1996;32(4):2990–3.
9. Eyssa YM, M Eyssa YM, Markiewicz WD. Quench simulation and thermal diffusion in epoxy impregnated magnet system. IEEE Trans Appl Supercond 1995;5(2):487–90.
10. Eyssa YM, Markiewicz WD, Miller J. Quench, thermal and magnetic analysis computer code for superconducting solenoids. IEEE Trans Appl. Supercond 1997;7(2):159–62.
11. Bottura L., Zienkiewicz OC. Quench analysis of large superconducting magnets. Part I: model description. Cryogenics 1992;32(8):719–28.
12. Bottura L., Zienkiewicz OC. Quench analysis of large superconducting magnets. Part II: model validation and application. Cryogenics 1992;32(7):659–67.
13. Thea. User's Guide. CryosSoft. Version 2.1; 2010.
14. Heater. User's Guide. CryoSoft. Version 2.0; 2010.
15. SuperMagnet. User's Guide. Cryosoft. Version 1.0; 2007
16. Numerical computation of internal and external flows. John Wiley and Sons; 1988.
17. Bajas H.., *et al.*, Quench analysis of high current density Nb3Sn conductors in a racetrack coil configuration. To be published. (Applied Superconductivity Conference 2014, IEEE trans. Appl. Superc.).
18. Bottura L, Bordini B. Jc(B,T,ϵ) Parametrization for the ITER Nb_3Sn Production. IEEE Transaction on Applied Superconductivity, vol. 19, no. 3, June 2009.
19. S. Russenschuck. ROXIE - A computer code for the integrated design of accelerator magnets.